原发性肾脏神经内分泌肿瘤的CT和MRI表现

王睿婷[1,2] 丁玉芹[1,2] 钟莲婷[3] 唐启瑛[3] 冒 炜[1,2] 戴辰晨[1,2] 曾蒙苏[1,2] 周建军[3,4△]

([1]上海市影像医学研究所 上海 200032;[2]复旦大学附属中山医院放射科 上海 200032;
[3]复旦大学附属中山医院厦门医院放射科 厦门 361015;[4]厦门市恶性肿瘤综合治疗临床医学研究中心 厦门 361015)

【摘要】 目的 探讨原发性肾脏神经内分泌肿瘤(primary renal neuroendocrine tumor,PRNET)的CT和MRI特征,以提高对该罕见病变的诊断水平。**方法** 回顾性分析8例经病理证实的PRNETs,4例行CT扫描,3例行MRI扫描,1例同时行CT和MRI扫描,总结其影像学特征,并与病理进行对照分析。**结果** 8例PRNETs中,6例分化良好,G1和G2级各3例,分化差的G3级2例;双肾各4例,病灶平均直径(4.1±1.7) cm,范围2.0~7.0 cm;类圆形5例,形态不规则3例;囊变4例,出血6例,坏死2例,钙化0例。1例位于肾上极,7例位于肾门附近。分化良好的PRNETs淋巴结转移1例,脉管癌栓1例。1例分化差的PRNET伴脉管癌栓、肝脏、骨及淋巴结多发转移。CT平扫均呈稍高密度,分化良好的PRNETs实质部分T1WI 3例等信号,1例高信号;T2WI 1例等信号,3例稍低信号;4例ADC图均呈低信号。分化良好的PRENTs增强后呈中度及明显强化,分化差的PRNETs轻中度强化,其中7例呈持续性强化,1例"快进快出"强化。**结论** PRNETs影像学表现有一定特征性,好发于肾门附近,CT平扫呈稍高密度,T2WI呈等或稍低信号。分化良好的PRNETs易囊变,增强后中度及明显强化,分化差的PRNETs易出血、坏死,增强后轻中度强化。

【关键词】 肾脏; 神经内分泌肿瘤(NET); 体层摄影术,X线计算机; 磁共振成像
【中图分类号】 R445 **【文献标志码】** A **doi**:10.3969/j.issn.1672-8467.2023.02.006

CT and MRI findings in primary renal neuroendocrine tumors

WANG Rui-ting[1,2], DING Yu-qin[1,2], ZHONG Lian-ting[3], TANG Qi-ying[3], MAO Wei[1,2], DAI Chen-chen[1,2], ZENG Meng-su[1,2], ZHOU Jian-jun[3,4△]

([1]*Shanghai Institute of Medical Imaging, Shanghai* 200032, *China*; [2]*Department of Radiology, Zhongshan Hospital, Fudan University, Shanghai* 200032, *China*; [3]*Department of Radiology, Zhongshan Hospital (Xiamen Branch), Fudan University, Xiamen* 361015, *Fujian Province, China*; [4]*Xiamen Clinical Research Center for Cancer Therapy, Xiamen* 361015, *Fujian Province, China*)

【Abstract】 Objective To investigate the CT and MRI features of primary renal neuroendocrine tumor (PRNET) in order to improve the diagnostic level of this rare disease. **Methods** Eight cases of PRNETs confirmed by pathology were retrospectively analyzed, of which, 4 cases underwent CT scan, 3 cases underwent MRI scan, and 1 case underwent both CT and MRI scans. The imaging characteristics were summarized and compared with pathology. **Results** Among the 8 PRNETs, 6 cases were well-differentiated, graded as G1 (n=3) and G2 (n=3), 2 cases were poorly-differentiated, graded as G3. Four lesions were located in the left kidney and the other four lesions were located in the right kidney, with an average diameter of (4.1±1.7) cm, ranging from 2.0 cm to 7.0 cm. There were 5 cases of round shape, 3 cases of irregular shape, 4 cases of cystic degeneration, 6 cases of hemorrhage, 2 cases of necrosis, and 0

福建省科技计划引导性项目(2019D025);福建省卫生健康科研人才培养项目医学创新课题(2019CXB33)
△Corresponding author E-mail: zhoujianjunzs@126.com
网络首发时间:2023-03-13 11:37:20 网络首发地址:https://kns.cnki.net/kcms/detail/31.1885.R.20230310.1137.010.html

case of calcification. One lesion was located at the upper pole of the kidney, and 7 cases were located near the renal hilum. One case of well-differentiated PRNETs showed lymph node metastasis, and 1 case of intravascular tumor thrombus, respectively. One case of the poorly-differentiated PRNETs demonstrated intravascular tumor thrombus, multiple metastases in the liver, bone and lymph nodes. All lesions showed slightly high attenuation on CT plain scan. Among the well-differentiated PRNETs, 3 cases showed iso-signal intensity (SI) and 1 case with high SI on T1WI. There was 1 case with iso-SI and 3 cases with slightly low SI on T2WI. All 4 lesions showed low SI on the ADC map. The well-differentiated PRENTs showed moderate and obvious enhancement, and the poorly-differentiated PRNETs showed mild to moderate enhancement after contrast enhancement, of which 7 cases showed continuous enhancement, and 1 case showed "wash-in and wash-out" enhancement. **Conclusion** The imaging findings of PRNETs have certain characteristics, usually located near the renal hilum, showing slightly high attenuation on plain CT scan, iso or slightly low SIs on T2WI. Well-differentiated PRNETs are prone to cystic degeneration, with moderate and obvious enhancement, while poorly-differentiated PRNETs are prone to hemorrhage and necrosis, and with mild and moderate enhancement.

【Key words】 kidney; neuroendocrine tumor (NET); tomography, X-ray computed; magnetic resonance imaging

*** This work was supported by Science and Technology Guided Project of Fujian Province (2019D025) and Health Scientific Research Cultivation and Medical Innovation Project of Fujian Province (2019CXB33).**

神经内分泌肿瘤(neuroendocrine tumor，NET)是一组起源于神经内分泌细胞的肿瘤，具有产生多肽类激素及活性胺的能力[1]。NET可发生于全身任何组织与器官，胃肠道、肺和胰腺为其好发部位，原发于肾脏者极为罕见，英文文献报道的肾脏NET约132例[2]，国内报道较少，仅见少量个案及病理分析。由于对该疾病的影像表现认识不足，术前明确诊断极其困难。本文回顾性分析复旦大学附属中山医院收治的8例原发性肾脏神经内分泌肿瘤(primary renal neuroendocrine tumors，PRNETs)的患者资料，总结其CT和MRI特征并与病理进行对照研究，旨在提高影像诊断水平。

资料和方法

一般资料 收集2010年8月—2021年8月复旦大学附属中山医院经病理证实的8例PRNETs的患者资料，其中男性3例，女性5例，年龄42～72岁，中位年龄52岁。2例患者有腹痛，余6例患者于体检时偶然发现。所有患者均行肾癌根治性切除术，术前1例误诊为肾上腺恶性肿瘤，1例误诊为乏脂肪血管平滑肌脂肪瘤，余6例诊断为肾脏恶性肿瘤。

检查方法 4例患者行CT扫描，3例患者行MRI扫描，1例患者同时行CT和MRI平扫+增强扫描。5例患者采用德国西门子SOMATOM Definition AS或SOMATOM Sensation CT扫描仪检查。患者取仰卧位，扫描范围自膈顶至髂嵴。管电压120 kV，管电流300～350 mA，层厚5 mm，螺距0.75。增强扫描对比剂采用碘海醇(300 mgI/mL)，以3～4 mL/s经肘静脉注射90 mL，皮髓交界期扫描采用CARE Dose 4D对比剂跟踪触发技术，触发阈值为腹主动脉100 HU，对比剂注射后80～90 s行肾实质期扫描。

4例患者采用德国Siemens Magnetom Aera 1.5T或Magnetom Verio 3.0T MRI扫描仪检查，平扫序列包括脂肪抑制快速自旋回波(turbo spin echo，TSE) T2WI；平面回波成像(echo planar imaging，EPI)的扩散加权成像(diffusion weighted imaging，DWI)，b=500 s/mm^{2}或800 s/mm^2；化学位移成像采用梯度自旋回波序列；T1WI平扫及多期增强扫描采用3D-VIBE(volumetric interpolated breath-hold examination)成像。层厚3～5 mm，间距1 mm。对比剂采用钆喷酸葡胺注射液(Gd-DTPA)，剂量为0.1 mmol/kg，总量30 mL，经肘静脉以2 mL/s流率注射。分别于对比剂注射后25～30 s、75～90 s、120～180 s行皮髓交界期、肾实质期

及排泄期扫描。

图像分析 由两名高年资放射科医师共同阅片并达成一致意见,观察肿瘤的部位、形态、大小、密度或信号、强化方式、强化程度、侵犯范围等特征。CT和MRI强化程度评判标准:以皮髓交界期为参照标准,肿瘤强化最明显处密度/信号低于肾髓质为轻度强化,高于肾髓质但低于肾皮质为中度强化,接近或超过肾皮质为明显强化[3]。

病理分析 PRNETs没有明确的病理分级系统,本研究采用2019 WHO关于消化道神经内分泌肿瘤的最新分级标准[4]:G1级:Ki-67指数<3%,核分裂相<2/10高倍镜视野(high power field,HPF);G2级:Ki-67指数在3%~20%,核分裂相在2~20/10 HPF;G3级:Ki-67>20%,核分裂相>20/10 HPF。

结 果

基本特征 患者基本特征见表1。8例PRNETs全部为单侧发病,双肾各4例,病灶最大径2.0~7.0 cm,平均直径(4.1±1.7) cm。5例呈类圆形,3例形态不规则;实性4例,实性为主3例,囊实性1例;囊变4例(图1、2),出血6例(图2A),坏死2例(图3),钙化0例。1例位于肾上极,余7例均位于肾门附近。2例G3级PRNETs病灶侵犯肾盂(图3),包绕肾门血管伴有同侧肾功能减退,边界不清。病例1病理有淋巴结转移,病例5伴有脉管内癌栓,病例8有右肾静脉癌栓、纵隔及腹膜后淋巴结转移、肝脏和骨多发转移。

表1 PRNETs患者的临床及影像学基本特征

Tab 1 Basic clinical and image features of PRNETs patients

Case number	Gender	Age (y)	Diameter (cm)	Region	Nature	Shape	Cystic degeneration	Hemorrhage	Necrosis	Calcification	Enhancement degree	Enhancement pattern	Grade
1	F	47	4.0	L	Mainly solid	Round	+	+	−	−	Moderate	Continuous	G1
2	F	56	6.0	R	Mainly solid	Round	+	−	−	−	Moderate	Continuous	G1
3	F	42	2.5	R	Solid	Round	−	−	−	−	Obvious	Continuous	G1
4	M	53	2.0	L	Mainly solid	Round	+	+	−	−	Obvious	Continuous	G2
5	F	51	3.5	R	Solid	Irregular	−	+	−	−	Moderate	Wash in and wash out	G2
6	F	51	4.5	L	Cystic solid	Round	+	+	+	−	Moderate	Continuous	G2
7	M	72	7.0	L	Solid	Irregular	−	+	+	−	Moderate	Continuous	G3
8	M	70	5.5	R	Solid	Irregular	−	+	−	−	Mild	Continuous	G3

F:Female;M:Male; L:Left; R:Right; −: Negative; + :Positive.

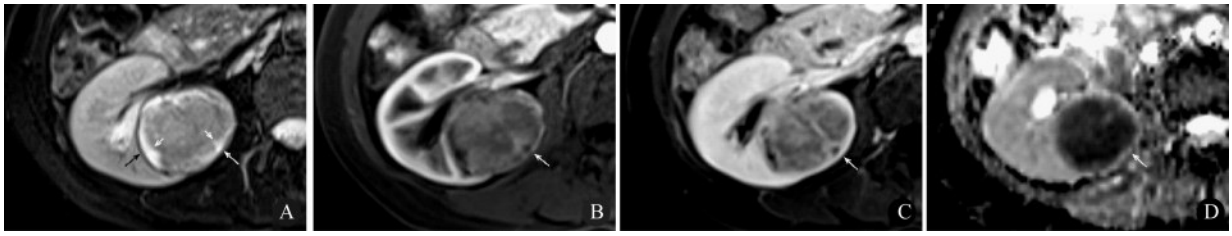

Female, 56 years old. A: T2WI showed a round mass near the right renal hilum (white long arrow) with slightly low signal in the solid portion and high signal in the cystic portion at the edge of the mass (white short arrow). It showed a clear boundary and circular low signal pseudocapsule around (black arrow); B: The mass showed mild to moderate enhancement in corticomedullary phase; C: It showed moderate persistent enhancement in nephrographic phase; D: ADC image showed obviously low signal(b = 500 s/mm^2).

图1 右肾类癌(G1级)的MRI表现

Fig 1 MRI manifestations of right renal carcinoid tumor (G1)

CT和MRI表现 CT平扫5例肿瘤实质部分均呈稍高密度（图2A、图3A），增强后皮髓交界期1例轻度强化，3例中度强化，1例明显强化（图2B），5例肾实质期均为持续强化。

平扫T1WI 1例呈稍高信号，3例呈等信号，T2WI 1例呈等信号，3例肿瘤实质部分呈稍低信号（图1A），其中1例可见环形低信号假包膜（图1A），4例DWI均为高信号，ADC图为低信号（图1D），4例正反相位均未见信号降低，增强后皮髓交界期2例中度强化，2例明显强化，肾实质期3例持续性强化（图1C），1例强化程度减退，呈“快进快出”强化。

病理学表现 根据核分裂相计数和Ki-67指数进行病理分级，分化好的PRNETs共6例，其中G1级（类癌）3例，G2级（不典型类癌）3例；分化差的G3级PRNETs 2例，其中1例为小细胞型。免疫组化8例肿瘤细胞对CD56、突触素（Syn）、嗜铬颗粒蛋白（CgA）的阳性表达分别为8/8、7/8和3/8。

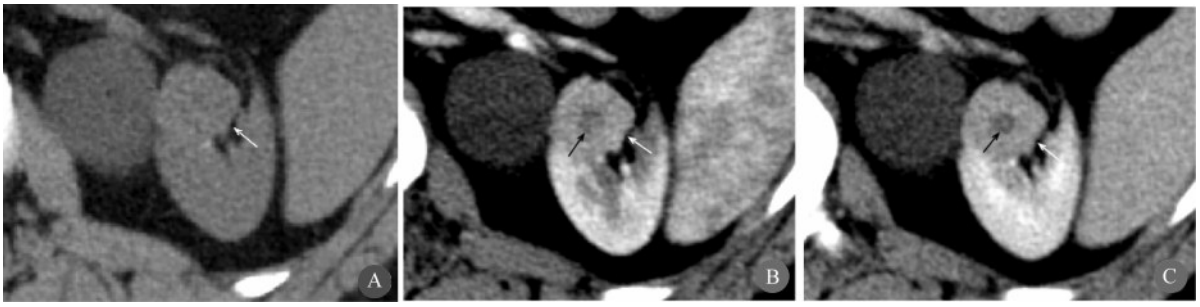

Male, 53 years old. A: CT plain scan showed a round and slightly high-density mass (CT value: 34 HU) (white arrow) with a clear boundary; B: It showed obvious persistent enhancement in corticomedullary phase (CT value: 85 HU) with a small non-enhanced cystic area in the center (black arrow); C: It showed continuous enhancement in nephrographic phase (CT value: 92 HU).

图2 左肾不典型类癌（G2级）的CT表现

Fig 2 CT manifestations of left renal atypical carcinoid tumor (G2)

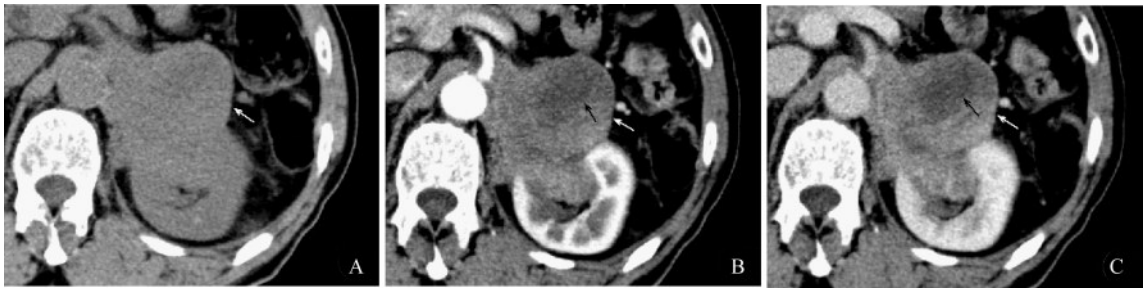

Male, 72 years old. A: CT plain scan showed an irregular mass (white arrow) with a unclear boundary in the left renal hilum. The solid portion of it showed slightly high density (CT value: 37 HU). It invaded the left renal pelvis and renal artery; B: It showed moderate inhomogeneous enhancement in corticomedullary phase (CT value: 67 HU) with patchy necrosis areas (black arrow); C: It showed continuous enhancement in nephrographic phase (CT value: 76 HU).

图3 左肾神经内分泌癌（G3级）的CT表现

Fig 3 CT manifestations of left renal neuroendocrine carcinoma (G3)

讨 论

临床及病理 NET组织学类型可分为分化良好（类癌和不典型类癌）与分化差（小细胞癌和大细胞癌）[2]。免疫组化检查可表达突触素（Syn）、嗜铬颗粒蛋白（CgA）、CD56及神经元特异性烯醇化酶等多种神经内分泌标志物，突触素是确诊NET最敏感的标志物[5]。PRNETs极为罕见，好发于50～60岁的中年人，无明显性别差异[6]，本组中位年龄为52岁，男女比例为3:5。大多数PRNETs患者无特殊临床表现，约12.7%分化良好的PRNETs患者可合并类癌综合征[6]，约17.8%的肾类癌可伴发马蹄肾[2]，分化差的PRNETs以腹痛、肉眼血尿最为常见[7]。本组PRNETs均未并发马蹄肾，2例患者有腹痛，余6例患者于体检时偶然发现。手术是PRNETs的首选治疗方法，分化良好的PRNETs恶性程度较低，不良预后因素包括年龄＞40岁，肿瘤

>4 cm、纯实性肿瘤、有丝分裂率超过1/10 HPF、肿瘤遍及肾包膜或发生转移[6]。分化差的PRNETs为高度恶性肿瘤,预后极差,约75%的患者在首次诊断后1年内死亡[8]。本组4例分化良好的PRNETs患者预后较好,未见复发及转移,余4例患者失访。

CT和MRI表现及病理基础 国内外关于PRNETs的影像学报道很少,分化良好的PRNETs常表现为境界清楚的实性肿块,并发马蹄肾者病灶多位于峡部附近,未并发马蹄肾者病灶多位于肾实质肾门附近[6]。分化差的PRNETs常表现为肾门附近边界不清的浸润性肿块[7]。分化良好的PRNETs钙化最为常见,发生率约26.5%,可伴有小灶性出血与囊变,而分化差的PRNETs可见大片坏死、易出血[7]。本组PRNETs中,病灶囊变仅见于4例分化良好的肿瘤,病灶出血见于4例分化良好、2例分化差的肿瘤,病灶坏死见于分化良好的和分化差的肿瘤各1例,与文献报道大致相符。但本组8例肿瘤均未见钙化,与文献报道不符,可能与样本量小有关。有研究认为钙化与肿瘤的惰性行为相关,而出血和坏死与肿瘤侵袭性生长、预后较差相关[6]。我们认为分化良好的PRNETs具有一定的神经内分泌功能,增殖缓慢可造成分泌物的沉积,因此囊变与钙化较为常见。而分化差的PRNETs肿瘤细胞分化程度低,增殖活跃,对微血管与实质侵犯能力较强,肿瘤微环境更易缺氧,因此出血与坏死较为常见。分化良好的PRNETs虽预后较好,据报道约50%的患者可发生转移,转移部位以区域淋巴结和肝脏多见[2]。分化差的PRNETs早期可发生淋巴结及远处器官转移,常侵及输尿管及脉管[9]。本组2例分化良好的PRNETs分别出现脉管内癌栓及淋巴结转移,2例分化差的PRNETs病灶侵犯肾盂、输尿管,其中1例就诊时已发生肝脏、骨、纵隔及腹腔淋巴结转移,与文献报道相符。

本组PRNETs在CT平扫上5例实质部分均呈稍高密度,与文献报道一致[6],在平扫T1WI上4例呈等或稍高信号,这可能与肿瘤细胞排列较为紧密、容易出血和分泌神经内分泌介质相关。本组4例分化良好的PRNETs在T2WI上呈等或稍低信号,其中1例可见假包膜,这可能由于肾脏本身血流较为丰富,含水量高,在T2WI上正常肾实质呈较高信号有关。据报道[10],分化差的PRNETs在T1WI上呈稍低信号,T2WI呈混杂信号,由于目前PRNETs的MRI影像学数据极少,因此需要更多的影像学数据进行补充印证。本组4例PRNETs在ADC图上均呈低信号,提示水分子弥散受限。有研究表明[11],分化差的胰腺神经内分泌肿瘤细胞增殖速度较快,细胞间隙更为紧密,核浆比值更大,水分子弥散受限更明显,ADC值与Ki-67指数呈负相关,我们推测ADC值与PRNETs的病理分级可能有一定的相关性。增强扫描后,本组6例分化良好的PRNETs表现为中度及明显强化,2例分化差的PRNETs表现为轻中度强化,与文献报道相符[7,12]。这可能由于分化良好的肿瘤间质血窦较为丰富,而分化差的肿瘤血管侵袭性更强,微血栓发生率高,从而导致动脉供血及静脉回流较少[13-14]。有研究表明,约75%的肾类癌增强后表现为轻度或无强化[6],与本组结果不同。本组7例病灶的强化程度随时相的延长不断提高,表现为“持续性强化”,与文献报道一致[12,15],这可能与PRNETs肿瘤细胞排列紧密,导致对比剂滞留有关。1例肾类癌表现为“快进快出”,这可能由于肿瘤间质富于薄壁血管,大量的薄壁血管对血流阻力较小,而肾髓质血流低且流速慢,因此造影剂通过瘤灶较快[7,16]。

鉴别诊断 分化良好的PRNETs需要与肾脏常见的富血供肿瘤鉴别。(1)肾透明细胞癌:CT平扫以低密度为主,T2WI通常为高信号,瘤周常见假包膜,部分病灶ADC图信号不低,易发生微囊变,增强后通常为明显强化,强化方式以“快进快出”为主。(2)肾嗜酸细胞腺瘤:常表现为边界清晰、血供丰富的肾脏实质性占位,部分病灶中心可见星芒状瘢痕和节段性强化反转,无局部浸润和远处转移征象。分化差的PRNETs需要与浸润性尿路上皮癌鉴别,两者均可表现为肾门区软组织肿块,增强后轻中度强化,易发生腹膜后淋巴结转移,伴有肾功能减低,前者主要为肾实质肿块侵犯肾盂,而后者会导致肾盂壁增厚,常伴有肾积水。

综上所述,PRNETs常表现为位于肾门附近的实性为主的肿块,CT平扫呈稍高密度,T2WI呈等或稍低信号,ADC图呈低信号,分化良好的PRNETs易囊变,增强后呈中度及明显强化,分化差的PRNETs易出血和坏死,增强后呈轻中度强化,随时间延长病灶呈持续性强化,但术前影像学诊断困难,具有上述征象时需要考虑有PRNETs的可能性。

作者贡献声明 王睿婷 数据采集和分析,论文构思和撰写。丁玉芹 论文构思、设计和指导。钟莲婷,唐启瑛,冒炜,戴辰晨 数据采集。曾蒙苏 论文审阅。周建军 研究方案可行性分析。

利益冲突声明 所有作者均声明不存在利益冲突。

参 考 文 献

[1] BARAKAT MT, MEERAN K, BLOOM SR. Neuroendocrine tumours[J].*Endocr Relat Cancer*, 2004, 11(1): 1-18.

[2] YI Z, LIU R, HU J, *et al*. Clinicopathologic features and survival outcomes for primary renal neuroendocrine neoplasms[J]. *Clin Genitourin Cancer*, 2021, 19(2): 155-161.

[3] SHINAGARE AB, DAVENPORT MS, PARK H, *et al*. Lexicon for renal mass terms at CT and MRI: a consensus of the society of abdominal radiology disease-focused panel on renal cell carcinoma [J].*Abdom Radiol (NY)*, 2021, 46(2): 703-722.

[4] ASSARZADEGAN N, MONTGOMERY E. What is new in the 2019 World Health Organization (WHO) classification of tumors of the digestive system: review of selected updates on neuroendocrine neoplasms, appendiceal tumors, and molecular testing [J].*Arch Pathol Lab Med*, 2021, 145(6): 664-677.

[5] ROSENBERG JE, ALBERSHEIM JA, SATHIANATHEN NJ, *et al*. Five new cases of primary renal carcinoid tumor: case reports and literature review [J].*Pathol Oncol Res*, 2020, 26(1): 341-346.

[6] ROMERO FR, RAIS-BAHRAMI S, PERMPONGKOSOL S, *et al*. Primary carcinoid tumors of the kidney[J].*J Urol*, 2006, 176(6 Pt 1): 2359-2366.

[7] 熊轶,张古田,樊祥山,等.肾脏原发性神经内分泌肿瘤五例报告并文献复习[J].中华泌尿外科杂志,2016,37(2):85-89.

[8] MAZZUCCHELLI R, MORICHETTI D, LOPEZ-BELTRAN A, *et al*. Neuroendocrine tumours of the urinary system and male genital organs: clinical significance [J].*BJU Int*, 2009, 103(11): 1464-1470.

[9] KATABATHINA VS, VIKRAM R, OLAOYA A, *et al*. Neuroendocrine neoplasms of the genitourinary tract in adults: cross-sectional imaging spectrum [J]. *Abdom Radiol (NY)*, 2017, 42(5): 1472-1484.

[10] KARADENIZ-BILGILI MY, SEMELKA RC, HYSLOP WB, *et al*. MRI findings of primary small-cell carcinoma of kidney[J].*Magn Reson Imaging*, 2005, 23(3): 515-517.

[11] 费莹,王明亮,温虹,等.表观弥散系数术前评估胰腺神经内分泌肿瘤病理分级的价值[J].中国临床医学,2021,28(5):864-868.

[12] 邓文娟,阳君.肾脏原发性小细胞神经内分泌癌1例[J].临床医学进展,2020,10(9):2068-2072.

[13] KARMAZANOVSKY G, BELOUSOVA E, SCHIMA W, *et al*. Nonhypervascular pancreatic neuroendocrine tumors: spectrum of MDCT imaging findings and differentiation from pancreatic ductal adenocarcinoma [J]. *Eur J Radiol*, 2019, 110: 66-73.

[14] GUO C, ZHUGE X, WANG Z, *et al*. Textural analysis on contrast-enhanced CT in pancreatic neuroendocrine neoplasms: association with WHO grade [J]. *Abdom Radiol (NY)*, 2019, 44(2): 576-585.

[15] CHEN Y, SHU Y, HE L, *et al*. Primary renal carcinoid tumors: three case reports[J].*Medicine (Baltimore)*, 2021, 100(8): e24714.

[16] 张秋峰.CT三期动态增强扫描在肾癌诊断中的临床价值研究[J].中国CT和MRI杂志,2018,16(4):107-109.

(收稿日期:2022-03-23; 编辑:王蔚)